Radar Cross Section:
Phase 1 Summary Report

Daniel Topa, ERT Inc.
AFRL/RVB
Kirtland AFB
Albuquerque, NM

April 20, 2020

Abstract

Currently the AFCAP dashboard represents just the mean radar cross section, the dominant term. The initiative is to expand the representation of the radar cross section for a more realistic characterization. Several reports have been submitted which record the progress and deliverables on the radar cross section analysis for HF radar using Mercury Method of Moments package. A brief synthesis of results follows, presenting an overview.

1 Stratagem

The overarching goal was to develop a process which starts with a FreeCAD model for an asset and produces a radar cross section (RCS) suitable for inclusion into the AFCAP dashboard. The current state of the art is a process nearly complete: we have created models, RCS profiles, and multiple representations of those profiles. But we have yet to experiment with putting these representations into the dashboard. However, there are fourl data compression formats and a reasonable hope is that at least one of them shall suffice.

Table 1: The challenge is to provide a richer RCS representation within the confines of browser capability.

Radar Cross Section	AFCAP dashboard
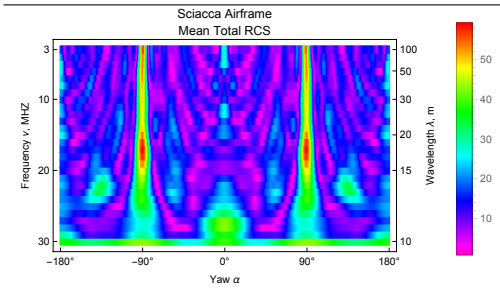	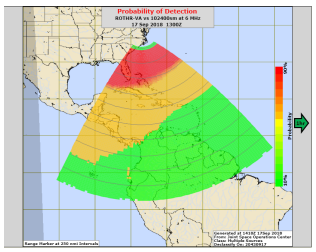

2 Accomplishments

To close the first phase of the project, we list process improvements and deliverables created for the project.

1. Streamlined Sciacca process
2. Replaced MATLAB/ALPINE scripts with Python scripts
3. Detailed simplifications in running Mercury MoM for the AFRL analysis
4. Quantified mesh tolerance of Mercury MoM
5. Produced automation tool for GUI use
6. Produced bash scripts for command line automation
7. Developed and explored strategies for data compression
   (a) Model decomposition
      i. Monomials (frequency variation)
      ii. Fourier (yaw variation)
   (b) Reduction
      i. Reduced sampling
      ii. Averaging

3 Process

3.1 Software tools: old and new

We were fortunate to build on the pioneering work of Capt. Joe Sciacca who showed us how to process a FreeCAD airplane tutorial model using Mercury Method of Moments (MoM)[1] to produce a radar cross section (RCS) profile. His contribution was more than a path forward; it also included explicit MATLAB scripts. With those scripts in hand, Chris McGeorge was quickly able to convert them to Python, thus relieving the need for a MATLAB license and access to the AFIT package ALPINE.

The process of *sealing the mesh*[2] was performed in the adjunct package MMViz. However, McGeorge noted that FreeCAD has a sophisticated mesh analysis and repair toolkit which Trevor Crawford mentioned is part of the active development gmsh open source project.

Schematically the process is shown in table 2 below.

Table 2: Overview of process of creating and processing a CAD model.

process:	CAD model	⇒	reformat	⇒	create RCS profile	⇒	plot
package:	FreeCAD	⇒	Python	⇒	MoM	⇒	Python
output file:	`*.obj`	⇒	`*.facet`	⇒	`*.4112.txt`	⇒	`*.png`

[1] Kam W. Hom, John Shaeffer, *Mercury Method of Moments and MMViz User's Guide*, NASA/LDTM—201502

[2] A process which insures there are no duplicate mesh points and that the mesh completely covers the surface with neither underlap nor overlap.

Table 3: How RCS measurements are organized according to radar frequency and yaw angle.

$$\begin{array}{cccc} \sigma_{\nu_1}(\alpha_1) & \sigma_{\nu_1}(\alpha_2) & \dots & \sigma_{\nu_1}(\alpha_n) \\ \sigma_{\nu_2}(\alpha_1) & \sigma_{\nu_2}(\alpha_2) & \dots & \sigma_{\nu_2}(\alpha_n) \\ \vdots & \vdots & \vdots & \vdots \\ \sigma_{\nu_m}(\alpha_1) & \sigma_{\nu_m}(\alpha_2) & \dots & \sigma_{\nu_m}(\alpha_n) \end{array}$$

Table 4: Extending table 3 to include another interrogation angle. Incorporating p angular samples would entail creating p instances of this file.

$$\begin{array}{cccc} \sigma_{\nu_1}(\alpha_1,\beta_1) & \sigma_{\nu_1}(\alpha_2,\beta_1) & \dots & \sigma_{\nu_1}(\alpha_n,\beta_1) \\ \sigma_{\nu_2}(\alpha_1,\beta_1) & \sigma_{\nu_2}(\alpha_2,\beta_1) & \dots & \sigma_{\nu_2}(\alpha_n,\beta_1) \\ \vdots & \vdots & \vdots & \vdots \\ \sigma_{\nu_m}(\alpha_1,\beta_1) & \sigma_{\nu_m}(\alpha_2,\beta_1) & \dots & \sigma_{\nu_m}(\alpha_n,\beta_1) \end{array}$$

3.2 Data format

The exercise establishes the capability to harvest data from ASCII files in tabular format.[3] For example, table 3 shows an organization of a computation of mean total cross section measurements σ for m different radar frequencies with n yaw samples: The idea extends naturally to adding another angular sweep[4] in pitch, or elevation. For p elevation samples there would p copies of this file in the format of table 4.

4 Data Compression

Computational limitation in the browser format of the AFCAP dashboard compels a search for data compression techniques, and we explored two categories: *modal decomposition* and *data reduction.*

4.1 Modal decomposition

The concept of a modal decomposition is to express a sequence of measurements in terms of modes of a aptly chosen set of basis functions. The set of basis functions is determined by the domain, the topology, and properties of the data.

Think of the modal decompositions as espousing two views of the data set: one as a set of rows (fixed radar frequency), the other as a set of columns (fixed yaw angle). These very different paradigms will require very different tools.

4.1.1 The problem determines the options

For example, for a fixed radar frequency, MoM outputs electric field values in equal increments about the unit circle. For the unit circle, the trigonometric functions e^{ikx} are a powerful choice

[3] Certainly binary files would be a better format.

[4] For modal decomposition development would extend naturally from the trignometric polynomials to the spherical harmonic functions.

as they are orthonormal in both continuous and discrete topologies:[5]

$$\left\{e^{ikx}\right\}_{k=0}^{d} = 1, \sin x + i\cos x, \sin 2x + i\cos 2x, \ldots, \sin dx + i\cos dx.$$

Another strategy involves fixing the yaw angle and letting the radar frequency vary. The interval is some bounded domain, for example HF radar frequencies in MHZ, $3 \leq \nu \leq 30$. Because the topology is discrete, we cannot use orthogonal functions, like those of Legendre. A wise choice would be the monomial, or Taylor, basis

$$1 \cup \left\{x^k\right\}_{k=1}^{d} = 1, x, x^2, \ldots, x^d.$$

To preclude esoteric arguments about near–orthogonality, we simply note the the monomial basis is affine–equivalent to the orthogonal polynomial basis of your choice.

To standardize the comparison, the two different modal representations will be Fourier,

$$\sigma_\nu \approx a_0 + a_1\cos\alpha + a_2\cos 2\alpha + a_3\cos 3\alpha + a_4\cos 4\alpha + a_5\cos 5\alpha + a_6\cos 6\alpha + a_7\cos 7\alpha,$$

and monomial,

$$\sigma_\alpha \approx a_0 + a_1\nu + a_2\nu^2 + a_3\nu^3 + a_4\nu^4 + a_5\nu^5 + a_6\nu^6 + a_7\nu^7.$$

4.1.2 Fourier basis

Consider the data when radar frequency is fixed and the yaw angle sample constitute an equipartition of the unit circle. Because of the symmetry of the object, the data is 2π periodic. Also, the periodicity and the integral equation operations within Mercury MoM insure the data is continuous. We are now within the realm of the Weierstrass Approximation Theorem and are assured uniform convergence over the domain. In terms of functional approximation, this is the gold standard. Furthermore, at wavelengths of 10 m, many targets posses bilateral symmetry which allows for a computations solely with even functions which cuts the representation in half.

Consider a typical result for $\nu = 3$ MHz, and $\alpha = 1, 2, 3, \ldots, 359$ as shown in table 5. The fit is quite good and requires eight amplitudes. The tight coupling between data and solution are a visual statement of the power of uniform convergence. The residual errors evince the tell-tale contributions of odd-functions added by Mercury MoM, and the scale of the errors shows their rather small contribution.

The next round of plots, in table 6, tell an interesting story about the composition of the RCS. The bar chart quickly tells a dominance hierarchy. The biggest contribution is from the mean, a_0. Therefore, thinking in terms of the current AFCAP implementation, the mean is the dominant term and the first term in an expansion, and the goal is to stir in other terms. Next, the even modes dominant the odd modes. The importance of subsequent terms is descreasing the gentle manner expected of an l^2 expansion of a continuous function.

The second plot with the error bars indicates that the amplitudes are well–characterized and stable against perturbations of the data. The numeric values for the amplitudes given in table 4.1.2.

The stated solution would then be

$$\begin{aligned}\sigma_{\nu=3}(\alpha) \approx & 35.237 + 1.675\cos\alpha - 3.434\cos 2\alpha \\ & - 0.866\cos 3\alpha + 5.368\cos 4\alpha - 1.280\cos 5\alpha \\ & + 1.379\cos 6\alpha - 0.367\cos 7\alpha.\end{aligned} \tag{1}$$

[5] By way of caution, note the blemish in the Sciacca procedure which precluded an orthogonal formulation. In that case, the solution was to continue to use the basis functions, e^{ikx}, yet fall back to their linear independence which does not depend upon the sampling mesh.

Table 5: The first plot shows the data points (purple) plotted against the solution curve.

Data points and solution	Residual errors

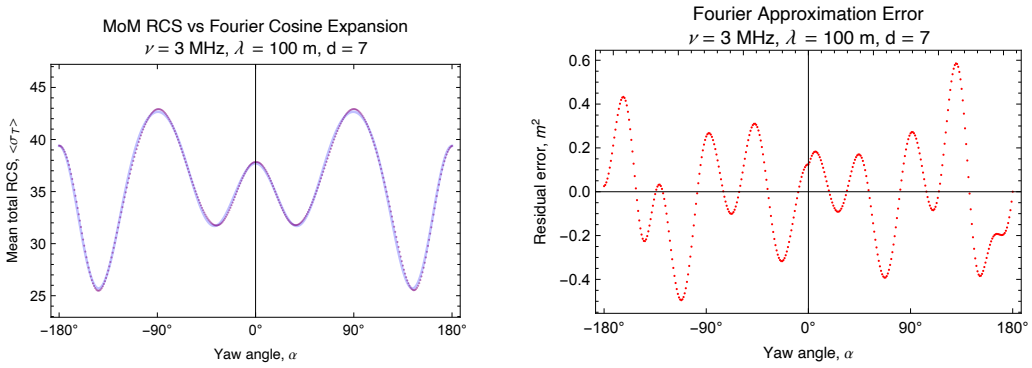

Table 6: The provides a visual guide of the size of each contribution, the second plot a quantification of the quality of the result.

Fourier amplitudes	Fourier amplitudes with error bars

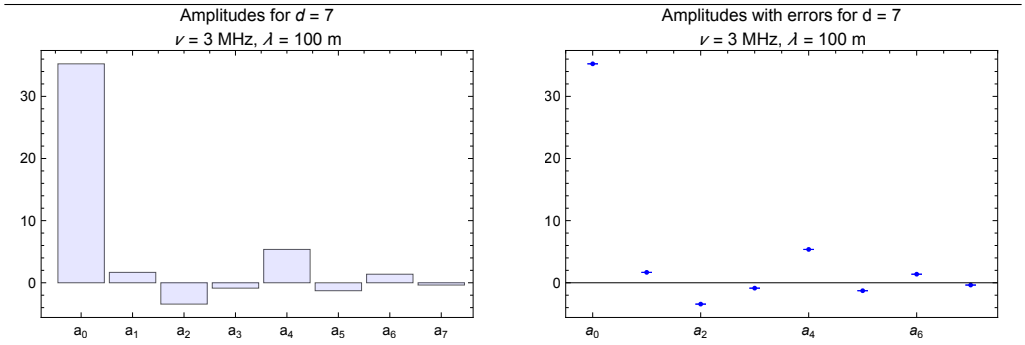

What is the economy of this method? In short, the 360 measurements have been encoded with eight numbers. The high resolution terms may demand additional terms. But for conversational purposes, this is a $45 - 1$ reduction.

4.1.3 Monomial or Taylor basis

The next strategy is to fix the yaw angle and capture the RCS variation with frequency. There is no periodicity to rely upon (behavior at very small frequencies will not match behavior at very large frequencies). The theorem of Weierstrass will not apply, and convergence is not uniform across the domain. We expect the fitting process to be less faithful and more challenging in a computational sense. While we escape the textbook problems of poor conditioning caused by the Vandermonde matrix by using a low-order expansion, other problems will manifest.

Consider a typical fit, here looking at the target nose-on (yaw $= 0°$), shown in table 8.

Table 7: Numeric values of the Fourier amplitudes, respecting significant digits. The set spans two orders of magnitude.

$$\begin{array}{rcrcr} a_0 & = & 35.237 & \pm & 0.012 \\ a_1 & = & 1.675 & \pm & 0.018 \\ a_2 & = & -3.434 & \pm & 0.018 \\ a_3 & = & -0.866 & \pm & 0.018 \\ a_4 & = & 5.368 & \pm & 0.018 \\ a_5 & = & -1.280 & \pm & 0.018 \\ a_6 & = & 1.379 & \pm & 0.018 \\ a_7 & = & -0.367 & \pm & 0.018 \end{array}$$

Table 8: The first plot for the monomial decomposition shows the data points (purple) plotted against the solution curve.

Data points and solution	Residual errors

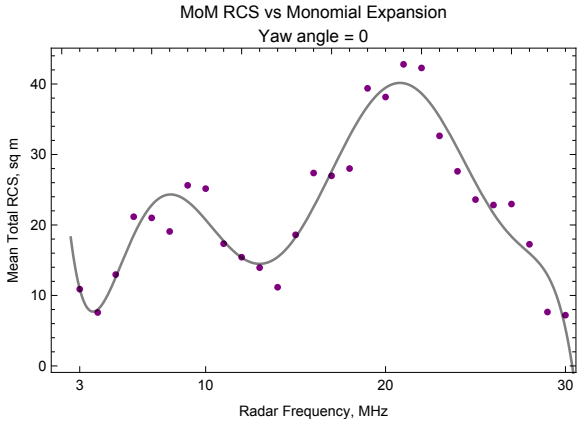

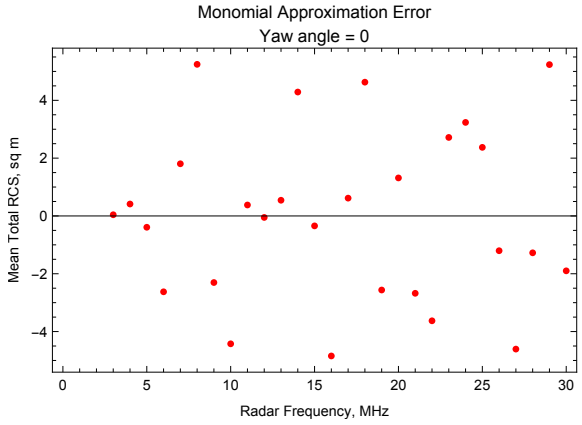

Notice the fit to the data is looser, and the residual errors are much larger.

The second plot with the error bars indicates that while the amplitudes are well–characterized, the rapidly decreasing magnitudes suggest reducing the order of the fit. The plots are a signal of distress which encourage a lower order fit to avoid higher powers of the frequency. The numeric values for the amplitudes given in table 4.1.3 emphasize the fact that the coefficients must shrink rapidly as the power of the term grows larger.

The stated solution would then be

$$\sigma_{\alpha=0}(\nu) \approx 31 - 34\nu - 16.5\nu^2 - 3.15\nu^3 + 0.295\nu^4 - 0.0143\nu^5 + 000346\nu^6 - 0.000000331\nu^7 \tag{2}$$

What is the economy of the monomial method? In short, the 28 measurements have been encoded with eight numbers, a meager $3-1$ reduction. The summary at the end, table 13,

Table 9: The first plot shows the data points (purple) plotted against the solution curve.

Monomial amplitudes	Monomial amplitudes with error bars
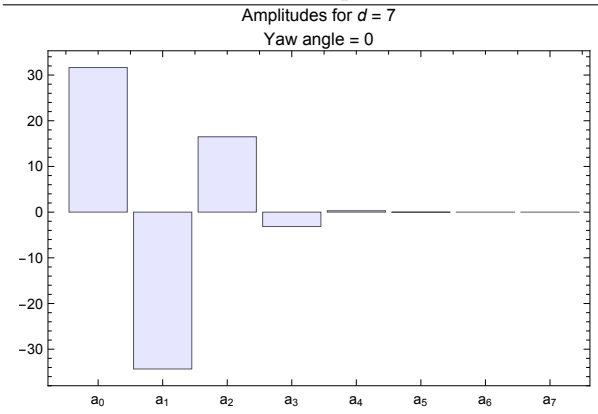	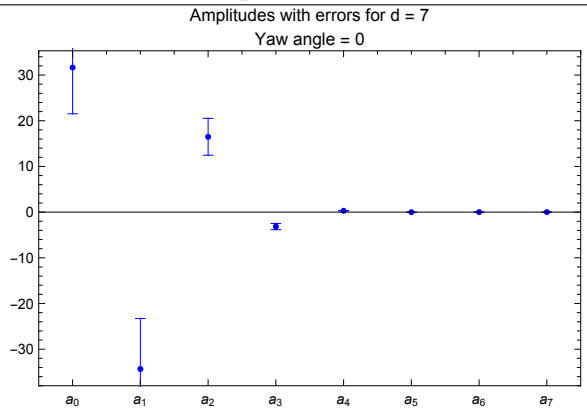

Table 10: Numeric values of the monomial amplitudes, respecting significant digits. The coefficients span six orders of magnitude.

a_0	=	31.	±	10.
a_1	=	−34.	±	11.
a_2	=	16.5	±	4.0
a_3	=	−3.15	±	0.68
a_4	=	0.295	±	0.060
a_5	=	−0.014	±	0.0029
a_6	=	0.000346	±	0.000071
a_7	=	−0.0000331	±	0.0000070

looks at reducing the angular measurements by power of 2 to boost the economy.

4.2 Reduction

The most basic tools for reducing the amount of data are *averaging* and *sampling*. While average *combines* information, sampling *ignores* information. Certainly when the number of samples is large and the averaging window is small, the methods look equivalent. However, averaging provides more information than sampling for the same data count.

The averaging method starts with a high–resolution MoM profile where measurements are made for every degree. Then the measurements are combined by computing the mean. For example, to combine three measurements at 1° increments starting at α°, use the prescription

$$\tilde{\sigma}\left(\alpha_{(k+2)/3}\right) = \frac{1}{3}\left(\sigma\left(\alpha_k\right) + \sigma\left(\alpha_{k+1}\right) + \sigma\left(\alpha_{k+2}\right)\right) \tag{3}$$

On the other hand, sampling would only use measurements at $1^\circ, 4^\circ, 7^\circ, \ldots, 357^\circ$.

The tables below, 11 and 12 provide a subjective visual comparison of the two reduction techniques using the color scale for the full data set in table 1.

Table 11: Data reduction via averaging.

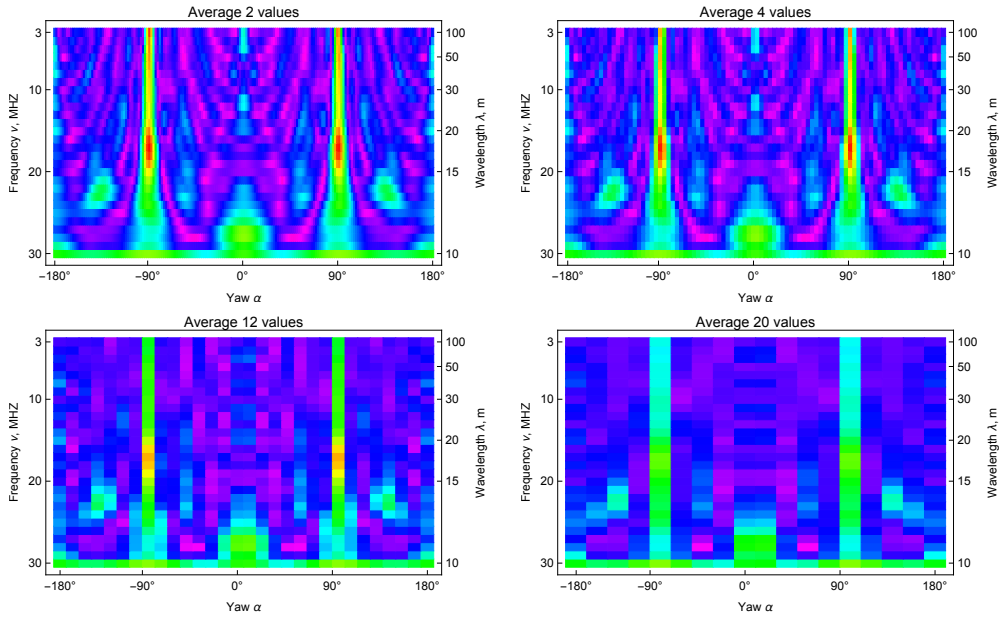

5 Ranking the Strategies

There are a few important subjective quality measures which have been discussed in the background reports. A crude yardstick for comparison is the *information content*, which counts the number of real variables needed to encode the information. The baseline, the Sciacca procedure featured 28 radar frequencies at 360 different angles. Therefore the information content is

$$28 \times 360 = 10,080.$$

Table 13 compares the information content of the various strategies for representing RCS information.

A careful review of the table nominates the Fourier representation as the most economical method to represent the RCS data.

Table 12: Data reduction via sampling.

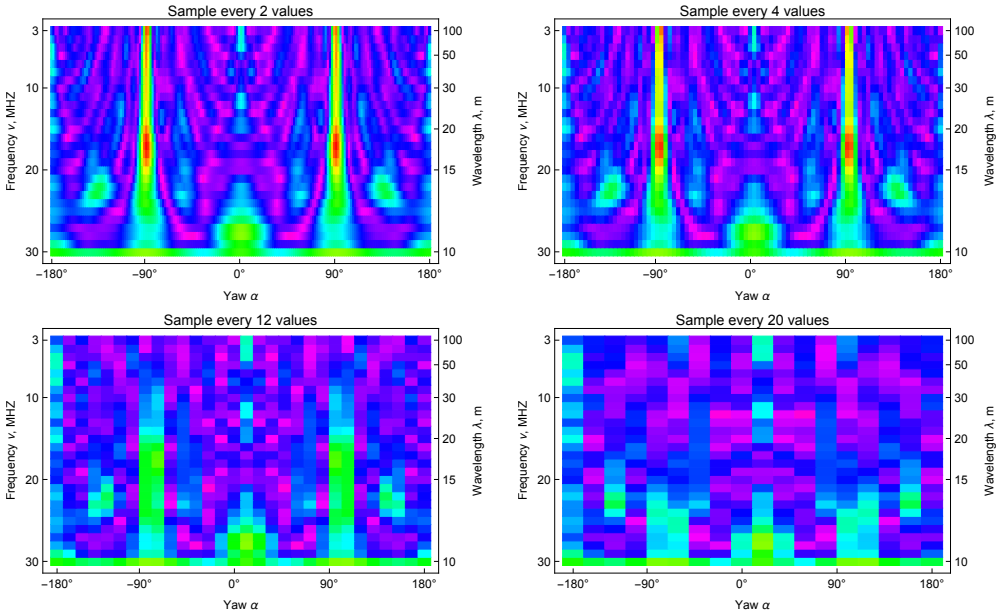

Table 13: Data budgets. Comparing the number of real variables needed to encode a representation. Smaller numbers are more favorable.

Count	method
10,080	raw data
5,040	Average 2 consecutive measurements (180 angles)
3,360	Average 3 consecutive measurements (120 angles)
2,880	Naive **monomial** fit at every degree
2,520	Average 4 consecutive measurements (90 angles)
2,016	Average 5 consecutive measurements (72 angles)
1,680	Average 6 consecutive measurements (60 angles)
1,440	Average 8 consecutive measurements (45 angles)
1,440	**Monomial** fit every two degrees
1,260	Average 9 consecutive measurements (40 angles)
1,120	Average 10 consecutive measurements (36 angles)
1,008	Average 12 consecutive measurements (30 angles)
840	Average 15 consecutive measurements (24 angles)
720	**Monomial** fit every four degrees
672	Average 18 consecutive measurements (20 angles)
560	Average 20 consecutive measurements (18 angles)
504	Average 20 consecutive measurements (18 angles)
360	**Monomial** fit every eight degrees
244	**Fourier representation** with eight terms
360	**Monomial** fit every 16 degrees